Nuclear Inst. and Methods in Physics Research, A 1052 (2023) 168308

Contents lists available at ScienceDirect

Nuclear Inst. and Methods in Physics Research, A

journal homepage: www.elsevier.com/locate/nima

Full Length Article

Neutron irradiation of Hydrogenated Amorphous Silicon p-i-n diodes and charge selective contacts detectors

M. Menichelli [a,*], M. Bizzarri [a,b], M. Boscardin [c,d], L. Calcagnile [e], M. Caprai [a], A.P. Caricato [e], G.A.P. Cirrone [f], M. Crivellari [d], I. Cupparo [g], G. Cuttone [f], S. Dunand [h], L. Fanò [a,b], B. Gianfelici [a,b], O. Hammad [d], M. Ionica [a], K. Kanxheri [a,b], M. Large [j], G. Maruccio [e], A.G. Monteduro [e], F. Moscatelli [a,i], A. Morozzi [a], A. Papi [a], D. Passeri [a,k], M. Pedio [a,i], M. Petasecca [j], G. Petringa [f], F. Peverini [a,b], G. Quarta [e], S. Rizzato [e], A. Rossi [a,b], G. Rossi [a], A. Scorzoni [a,k], L. Servoli [a], C. Talamonti [g], G. Verzellesi [c,l], N. Wyrsch [h]

[a] INFN, Sez. di Perugia, via Pascoli s.n.c. 06123 Perugia, Italy
[b] Dip. di Fisica e Geologia dell'Università degli Studi di Perugia, via Pascoli s.n.c. 06123 Perugia, Italy
[c] INFN, TIPFA, Via Sommarive 14, 38123 Povo (TN), Italy
[d] Fondazione Bruno Kessler, Via Sommarive 18, 38123 Povo (TN), Italy
[e] INFN and Dipartimento di Matematica e Fisica "Ennio de Giorgi" dell'Università di Lecce, Via per Arnesano, 73100 Lecce, Italy
[f] INFN Laboratori Nazionali del Sud, Via S. Sofia 62, 95123 Catania, Italy
[g] INFN and Dipartimento di Fisica e Astronomia dell'Università di Firenze, Via Sansone 1, 50019 Sesto Fiorentino (FI), Italy
[h] Ecole Polytechnique Fédérale de Lausanne (EPFL), Institute of Electrical and Microengineering (IME), Rue de la Maladière 71b, 2000 Neuchâtel, Switzerland
[i] CNR-IOM, via Pascoli s.n.c. 06123 Perugia, Italy
[j] Centre for Medical Radiation Physics, University of Wollongong, Northfields Ave Wollongong NSW 2522, Australia
[k] Dip. di Ingegneria dell'Università degli studi di Perugia, via G. Duranti 06125 Perugia, Italy
[l] Dip. di Scienze e Metodi dell'Ingegneria, Università di Modena e Reggio Emilia, Via Amendola 2, 42122 Reggio Emilia, Italy

ARTICLE INFO

Keywords:
Hydrogenated amorphous silicon detectors
Beam flux detectors
Particle detectors
X-ray detectors
Radiation damage
Solid state detectors

ABSTRACT

Hydrogenated amorphous silicon is a well-known detector material for its radiation resistance. For this reason it has been used in particle beam flux measurements and in solar panels designed for space applications. This study concern 10 μm thickness, p-i-n and charge selective contacts planar diode detectors which were irradiated with neutrons to two fluence values: 10^{16} n_{eq}/cm^2 and 5×10^{16} n_{eq}/cm^2. In order to evaluate their radiation resistance, detector leakage current and response to x-ray photons have been measured. The effect of annealing for performance recovery at 100 °C for 12 and 24 h has also been studied. The results for the 10^{16} n_{eq}/cm^2 irradiation show a factor 2 increase in leakage current that is completely recovered after annealing for p-i-n devices while charge selective contacts devices show an overall decrease of the leakage current at the end of the annealing process compared to the measurement before the irradiation. X-ray dosimetric sensitivity degrades, for this fluence, at the end of irradiation, but partially recovers for charge selective contact devices and increases for p-i-n devices at the end of the annealing process. Concerning the 5×10^{16} n_{eq}/cm^2 irradiation test (for p-i-n structures only), due to the activation that occurred during the irradiation phase, the measurements were taken after 146 days of storage at around 0 °C, during this period, a self-annealing effect may have occurred. Therefore, the results after irradiation and storage show a noticeable degradation in leakage current and x-ray sensitivity with a small recovery after annealing.

1. Introduction

Radiation damage effects in Hydrogenated Amorphous Silicon (a-Si:H) have been extensively studied in the field of solar panels for Space applications [1–3]. Concerning the radiation resistance for the usage of this material in particle flux measurement, a fundamental reference paper is [4], where a 32 μm thick n-i-p diode has been used for a proton beam monitoring experiment at high fluences (up to about 10^{16} p/cm^2). The resulting increment in the leakage and responsivity degradation was completely reversed after 24 h of annealing in air at 100 °C.

* Corresponding author.
E-mail address: mauro.menichelli@pg.infn.it (M. Menichelli).

https://doi.org/10.1016/j.nima.2023.168308
Received 9 November 2022; Received in revised form 27 March 2023; Accepted 13 April 2023
Available online 20 April 2023

Although a-Si:H has such a remarkable radiation resistance, a planar detector fabricated using this material possesses a primary limitation in a poor signal-to-noise ratio for the detection of MIP (Minimum Ionizing Particle) that has yet to exceed the value of 5. The reason for this is the very high voltage needed to deplete a thick detector. The operating voltage increases as the square root of the thickness and typically exceeds 100 V for a 10 μm thick sample and generates a very high leakage current that can reach the order of 1 $\mu A/cm^2$, which increases the noise level; moreover, the charge collection efficiency is below 50% for a 10 μm thick diode, which reduces the signal amplitude.

In this study, two different types of devices were irradiated and tested: (a) p-i-n diodes fabricated using ion implantation of Phosphorous (n-type) or Boron (p-type) described in details in [5–7] and (b) Charge selective contact devices fabricated by sputtering of charge selective oxides: MoO_x for hole selective contacts and TiO_2 or Aluminum doped ZnO (AZO) for electron selective contacts described in [8]. In this paper, neutron irradiation testing data will be shown. The total displacement dose obtained with neutrons is similar, in the NIEL approximation, to the displacement dose of [4] that was obtained with protons. Moreover, the annealing procedure followed in this work is the same adopted in [4]. The main differences between the two measurements are (a) the thickness of the diode (10 μm for this study and 32 μm in [4]), (b) the type of damage: purely displacement damage here and a combination of total ionizing dose and displacement damage in [4], (c) the flux sensitivity measurement: flux measurements of protons in [4] and X-ray flux measurements for this paper. The present work shows a neutron radiation test with doses above 10^{16} $n_{eq(1MeV)}/cm^2$ performed on a-Si:H detectors. In this test, the dominant damaging mechanism is displacement damage. Subsequent proton radiation damage tests and total ionizing dose tests with X-rays will be performed and the results will be published in forthcoming papers. The data presented here were collected during a radiation test performed in the framework of the INFN HASPIDE experiment with the goal of fabricating devices on flexible substrate for beam monitoring, particle fluxes measurements in solar events and neutron flux measurements.

2. Tested devices and test procedure

Three different devices, having different geometries, have been irradiated during this irradiation session: (a) vertical p-i-n diode devices in square pad form. (b) vertical p-i-n diode devices in strip form (c) vertical charge selective contacts diodes in square pad form.

Configuration (a) is shown in Fig. 1a depicting a 3 × 2 diode array of p-i-n vertical diodes where a 10 μm layer of a-Si:H is deposited on a p-type crystalline Silicon low resistivity substrate (thickness of 300 μm). On the top of this layer the 6 n-i junctions having 0.5 × 0.5 mm^2 dimensions are fabricated via ion implantation (100 nm implantation depth) of phosphorous. Passivation with SiO_2 (160 nm deposited by Plasma Enhanced Chemical Vapor Deposition PECVD [8]) and diode metallization with chromium + aluminum (5 nm Cr + 500 nm Al) is added on the top of the device. The device is then packaged in a ceramic DIL Package (P/N: CSB02219 from Semi Spectrum, US).

Configuration (b) (shown in Fig. 1b) is an 8-strip device fabricated using the same process described for configuration (a), where the strips have dimensions 5 × 0.2 mm^2.

Configuration (c) (Fig. 1c) has 4 planar charge selective contact devices each having 4 × 4 mm^2 surface on a 8.2 μm thick a-Si:H substrate. Molybdenum oxide, adopted for hole selective contacts, is deposited on top of the device, just under the ITO (indium tin oxide) contact metallizations visible as blue squares in the picture, while the in the bottom of the device, the electron selective contact is obtained by deposition of aluminum-doped zinc oxide (AZO). These detectors have been described in [9].

The tests were performed according to the following procedure:

1. Pre-irradiation leakage current versus bias voltage measurements test and measured current versus dose rate for exposure to an x-ray tube biased at 30 kV at different tube currents. X-ray dose-rate versus tube current calibration procedure is described below.
2. Irradiation with neutrons of two separate detectors sets; each set has been irradiated at different fluences (see below)
3. Post irradiation measurements are basically a repetition of the test described at point 1 after irradiation.
4. Annealing in air (phase-1) of irradiated sample in an oven at 100 °C for 12 h.
5. Post phase-1 annealing measurements with the procedure described at point 1
6. Annealing in air (phase-2) of irradiated sample in an oven at 100 °C for an additional 12 h.
7. Post phase-2 annealing measurements with the procedure described at point 1.

The detectors have been irradiated with neutron at the Jozef Stefan Institute in Ljubljana (Slovenia) to two different fluences of 1 × 10^{16} $n_{eq(1MeV)}/cm^2$ and 5 × 10^{16} $n_{eq(1MeV)}/cm^2$, in two different batches.

The neutron spectrum used in this irradiation test is reported in Fig. 2, this spectrum is used in the calculation of the NIEL (Non-Ionizing Energy Loss). In order to obtain the fluence in units of 1 MeV neutron equivalent damage the results of this calculation it is divided by 2.037 keV cm^2/g which is the displacement damage dose of one neutron having 1 MeV kinetic energy in Silicon [10].

During the tests, we measured the leakage current at various bias voltages and the detector current under X-ray irradiation at different dose rates. The former is related to the long-term charge collection efficiency which is a useful quantity to determine the performance of devices when used in a beam monitoring application. From the linear fit of the x-ray irradiation data, we extracted the dosimetric sensitivity. The detectors were biased using a Keithley 2410-C and a Keithley 2400 SMU that measures currents with a resolution of 10 pA. X-rays were generated by a tube from Newton Scientific having 50 kV maximum voltage and 200 μA maximum current [12]. The doses were measured using a Cobia Flex dosimeter equipped with a RTI T20 dose probe [13].

The x-ray test setup in Perugia is shown in Fig. 3 and typical doses versus tube current calibration curve is shown in Fig. 4. This calibration aims to determine the correspondence between the x-ray flux generated by the current in the tube and the dose rate in the sample measured, employing the Cobia flex dosimeter probe placed in the same position of the irradiated detector device.

3. Results

3.1. Results after 10^{16} n/cm^2 irradiation.

We tested one configuration (b) and one configuration (c) device after 10^{16} n_{eq}/cm^2 neutron irradiation. The leakage current was measured for one p-i-n strip diode device and one charge selective contact device. In Fig. 5 the leakage current on p-i-n device is shown before and after irradiation and after 12 h of annealing at 100 °C as described in the previous chapter. The reason why we did annealing only for 12 h is due to a hardware problem with the oven that barred any further annealing until repair. Since the detector recovered its original leakage current and sensitivity (even with some improvement) already after 12 h annealing, we decided to go on without the data for sensitivity after 24 h annealing because the long period foreseen for the oven repair would also introduce a self-annealing that could alter the results. Measurements were performed 30 min after the device was placed under bias at the maximum voltage for device current stabilization

Compared to pre-irradiation values an increment of leakage current can be observed after irradiation, especially at bias voltages below 70

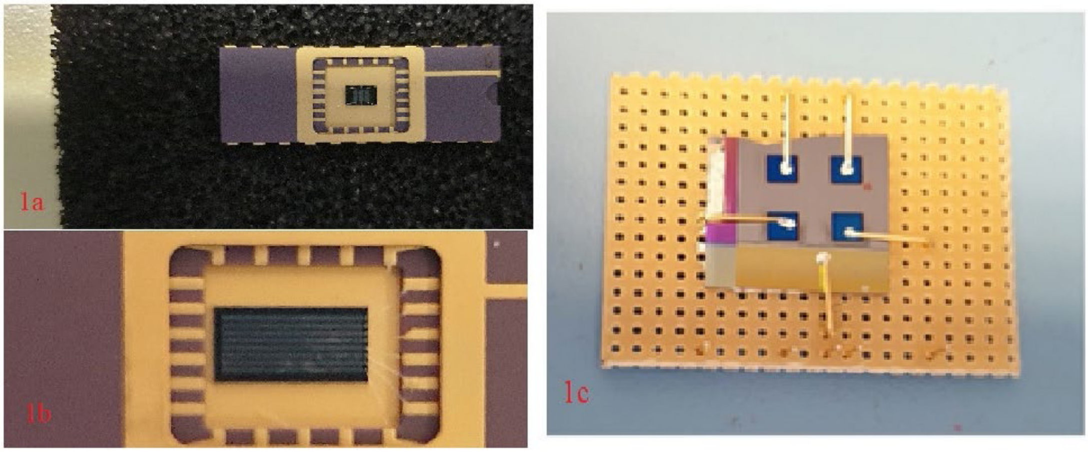

Fig. 1. Detector configurations tested for displacement damage (a) Configuration (a) 2 × 3 pad detector array with n junction implanted and is packaged on a ceramic package (b) configuration (b) 8 strip detector with n junction implanted. (c) Configuration (c) has 4 charge selective contact devices having 4 × 4 mm^2 surface and 8.2 μm a-Si:H thickness.

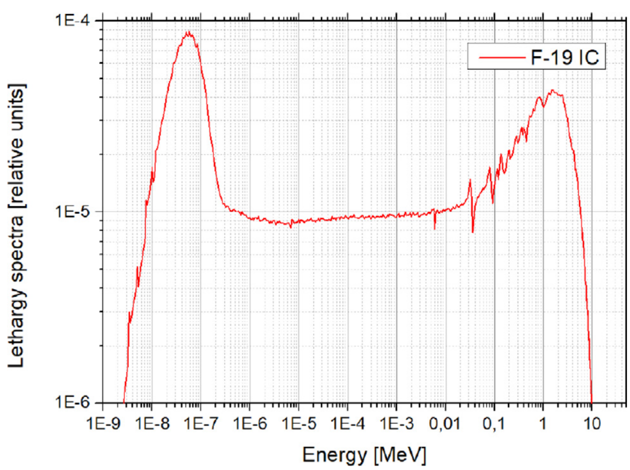

Fig. 2. Spectrum of neutron used in this irradiation test [11].

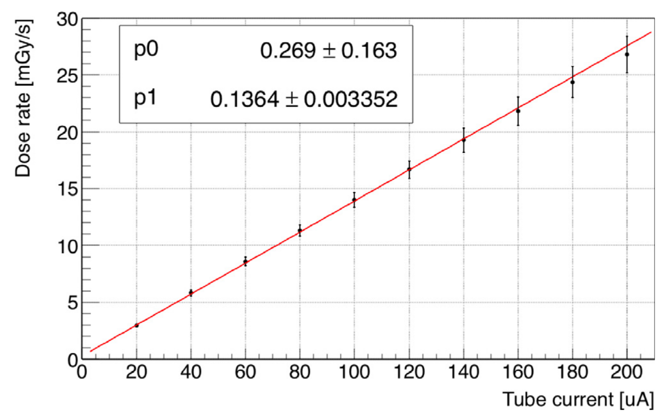

Fig. 4. Typical calibration curve between dose and tube current at 30 kV tube voltage. The dose rate was measured by a Cobia Flex dosimeter with the probe placed in the same position of the Device under test (DUT) irradiated at various tube currents.

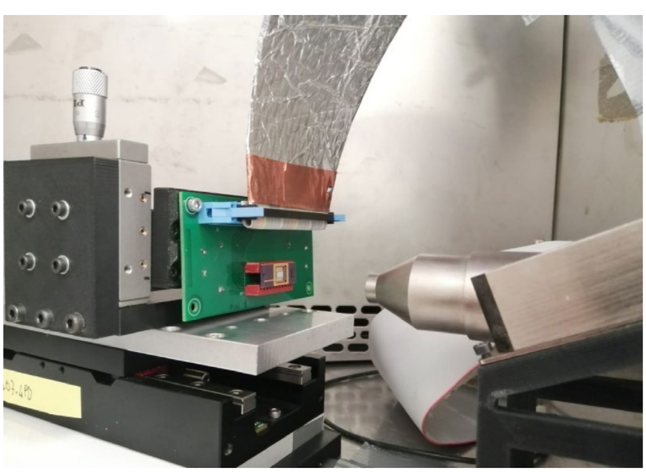

Fig. 3. Test setup for x-ray response measurement.

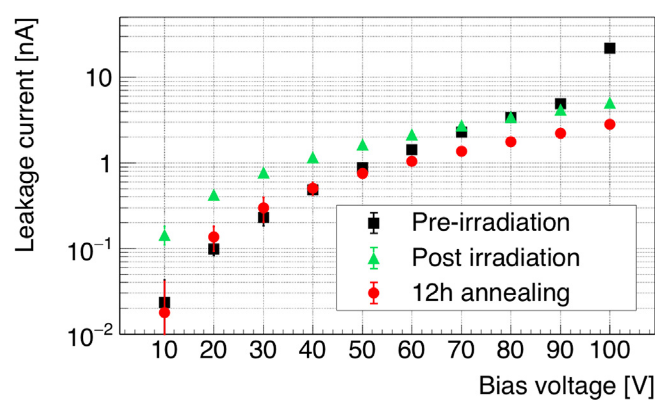

Fig. 5. Leakage current versus bias voltage for p-i-n device. The measurement where taken before and after neutron irradiation and after 12 h of annealing.

V. After 12 h of annealing, a new measurement was performed and leakage current returned to pre-irradiation values at low bias voltage, becoming even lower at bias voltages higher than 50 V. This is in agreement with what was observed for protons in [4]. The leakage current before irradiation, shows at $V_{bias} > 80$ V, the beginning of the onset of a breakdown behavior that disappear after irradiation due to a rearrangement of the local structure of the amorphous material.

The leakage current of charge selective devices was measured and it is shown in Fig. 6. Also in this case, we observe an increment of leakage current after the irradiation. The increment was higher at high values of the bias voltage and lower at low bias voltages. Two annealing sessions were performed lasting 12 h each at 100 °C.

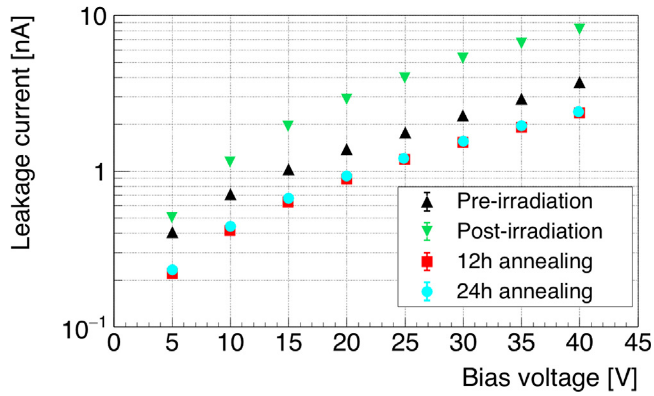

Fig. 6. Leakage current versus bias voltage for charge selective contacts device. The measurement were taken before and after neutron irradiation and after 12 and 24 h of annealing.

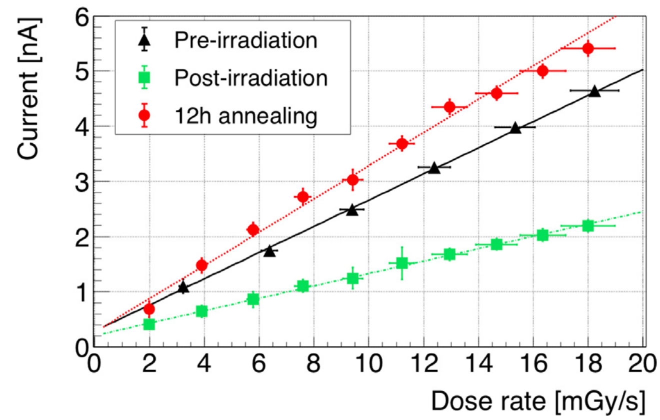

Fig. 7. P-i-n diode device response to x-ray irradiation versus dose rate. The measurement were taken before and after neutron irradiation and after 12 h of annealing at 100 °C.

After the first 12 h of annealing, the values of the leakage current at various voltages were lower than the pre-irradiation values. The additional 12 h annealing session did not result in any further decrease in leakage current. Due to the metastability of the material, without a proper pre-annealing step, the device is in an undefined state that depends on the various exposure history (light, irradiation, temperature) since its deposition or last full annealing. Therefore, without pre-annealing, it is not possible to know if the effect of the annealing can over-compensate the damage induced. This effect, although less evident, is also shown in [4].

Radiation sensitivity and flux response to x-ray irradiation have been measured for these detectors in order to study the response to x-rays and to demonstrate their capability to measure radiation fluxes under severe radiation environments. For this purpose, we used the setup shown in Fig. 2 with the tube biased at 30 kV and dose rates from 0 to 24 mGy/s.

The p-i-n diode device biased at 60 V gave the response shown in Fig. 7. The response was linear under all conditions and the sensitivity changed from 2.39 nC/cGy for the non-irradiated component to 1.13 nC/cGy after irradiation; after the 12 h of annealing the sensitivity increased up to 3.0 nC/cGy. This increment is somehow comparable with the leakage current behavior where the leakage current increases after irradiation and decreases below the pre-irradiation value after annealing. It is important to mention that the points of the graph in Fig. 7 are obtained by measuring the current under x-ray irradiation after subtracting the values of the leakage current. Errors in dose rate are evaluated from the uncertainty of the exact distance between the tube and the detector and for the errors on current we took the standard deviation of measured values.

Charge selective devices response to x-ray irradiation at various rates has been measured both at 0 V (photovoltaic mode typical of medical dosimeters) bias and 30 V bias (more suitable for beam monitoring); the results are shown in Figs. 8 and 9.

It is worth noting that, from these data, the recovery after irradiation is less evident than in the p-i-n diode device. The response is linear, especially when bias is applied; however, at 0 V the charge sensitivity is 0.86 nC/cGy for the non-irradiated component while after irradiation decreases by a factor of 8.6 (0.10 nC/cGy). The device partially recovers after 12 h of annealing up to 0.24 nC/cGy and to 0.30 after 24 h of annealing. The results obtained with a 30 V bias confirm this trend: the sensitivity before irradiation was 11.1 nC/cGy reduced by more than a factor 2 after neutron irradiation down to 5.0 nC/cGy, it partially recovers after 12 h annealing up to 6.5 nC/cGy and after 24 h up to 7.2 nC/cGy. A summary table of these results is shown in Table 1.

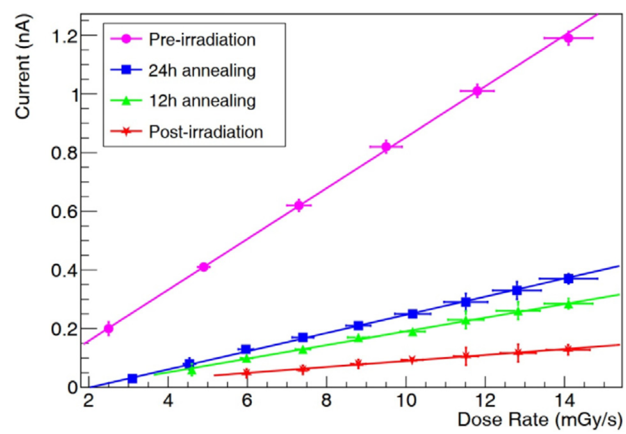

Fig. 8. Charge selective contacts device (at 0 V bias) response to x-ray irradiation versus dose rate. The measurement where taken before and after neutron irradiation and after 12 and 24 h of annealing at 100 °C.

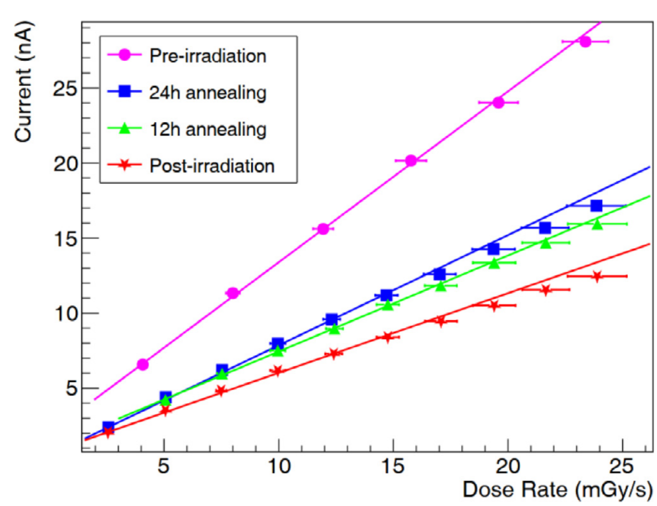

Fig. 9. Charge selective contacts device (at 30 V bias) response to x-ray irradiation versus dose rate. The measurement where taken before and after neutron irradiation and after 12 and 24 h of annealing at 100 °C.

Table 1
Sensitivity under various conditions for p-i-n diode and charge selective contacts devices after 10^{16} neq/cm^2 neutron irradiation.

Detector type and bias	Pre-rad Sensitivity (nC/cGy)	Sensitivity after irradiation (nC/cGy)	Sensitivity after 12h annealing (nC/cGy)	Sensitivity after 24h annealing (nC/cGy)
CSC at 30V bias	11.1 ± 0.3	5.0 ± 0.1	6.5 ± 0.2	7.2 ± 0.2
CSC at 0V bias	0.86 ± 0.03	0.10 ± 0.02	0.24 ± 0.02	0.30 ± 0.02
P-i-n diode at 60V	2.39 ± 0.09	1.13 ± 0.08	3.0 ± 0.1	-

3.2. Results after 5×10^{16} n_{eq}/cm^2 irradiation.

One configuration (a) and one configuration (b) p-i-n diode devices were irradiated to 5×10^{16} n_{eq}/cm^2 neutron fluence.

After the irradiation the components were heavily activated and measurements could only be carried out 146 days after the irradiation. Although during this time the components were kept at approximately 0 °C some self-annealing in air may have occurred. This effect can explain the reason why for this measurement the actual annealing at 100 °C had a reduced effect compared with the measurements described in the previous section. Due to residual radioactivity after irradiation the components could not be shipped, hence the x-ray response was measured after irradiation and annealing at the JSI laboratory with a different setup. The x-ray tube that was used in Ljubljana had a tungsten cathode, voltage in the 5–160 kV range with current in the range 0.5–50 mA and maximum power of 3 kW. Preliminary dosimetric measurements on the JSI setup were performed with the same instrument we used for the measurement described in the previous section for dose rate consistency of the two setups. A picture of the JSI x-ray setup is shown in Fig. 10.

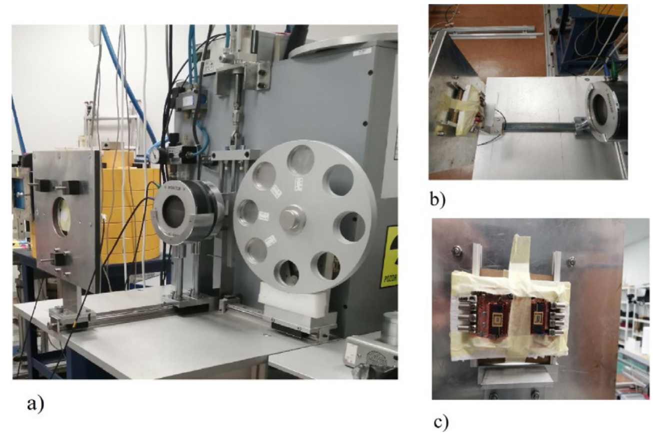

Fig. 10. (a) X-ray tube at JSI with monitoring ionization chamber and sample holder (b) Top view of ionization chamber and sample holder (c) samples on the holder irradiated simultaneously.

The leakage current for one of the configurations (a) devices is shown in Fig. 11. There is a relevant increase (by a factor of 2.5 at 100 V) in leakage current after irradiation that does not change after annealing likely due to self-annealing under storage as hypothesized at the beginning of this section. The larger error bars on the pre-irradiation curve are due to the different (and noisier) setup used.

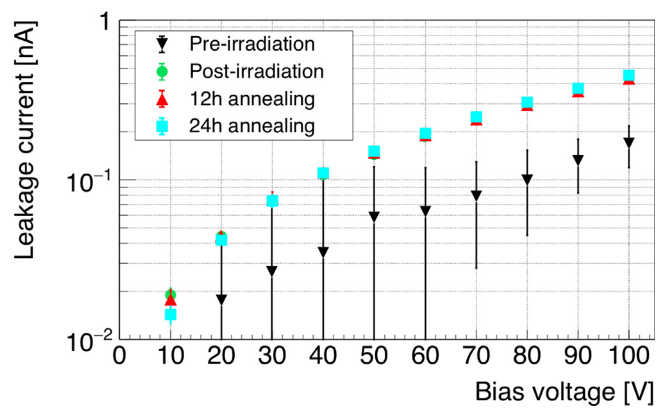

Fig. 11. Leakage current versus bias voltage for configuration (a) device. The measurements were taken before and after neutron irradiation and after 12 and 24 h of annealing.

Concerning the configuration (b) device (Fig. 12) we notice a decrease in leakage current after irradiation (and self-annealing). After the 12 h of annealing at 100 °C the leakage current increased above the non-irradiated values and did not change significantly after 12 additional hours of annealing. Also in this case, the leakage current at $V_{bias} > 80$ V shows in the unirradiated device the onset of a breakdown behavior that disappears after irradiation due to a rearrangement of the local structure of the amorphous material.

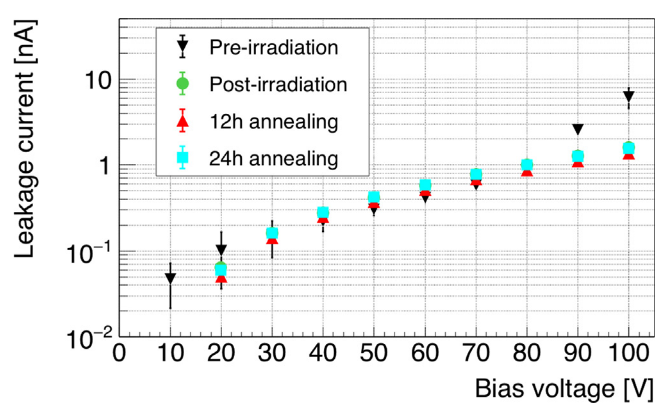

Fig. 12. Leakage current versus bias voltage for configuration (b) device. The measurements were taken before and after neutron irradiation and after 12 and 24 h of annealing.

X-ray response was measured for both devices. Configuration (a) device (Fig. 13) shows good linearity and a reduction of sensitivity from 1.94 to 0.57 nC/cGy after irradiation and self-annealing. After 12 h of annealing the sensitivity increased to 0.77 nC/cGy and after 24 h of annealing increased additionally up to 0.84 nC/cGy.

Additionally, configuration (b) device shows very good linearity (Fig. 14). After irradiation and self-annealing the charge sensitivity was reduced from 2.55 to 0.74 nC/cGy. After 12 h of annealing the sensitivity increased to 1.07 nC/cGy and after 24 h of annealing increased additionally up to 1.27 nC/cGy

A summary table of these measurements is shown in Table 2.

The fact that the complete recovery in leakage current does not correspond to a complete recovery in sensitivity in dev. (b) may be ascribed to the fact that although the correlation between charge sensitivity and leakage current actually exists (from the point of view of bulk defects generation and recovery) it is not always straightforward because also junction effects (metal-p, metal-n, n-i, p-i, CSC-i) comes into play, especially for the leakage currents of two devices, which differ in shape and area. We cannot give a definite answer to this fact and further investigations should be performed.

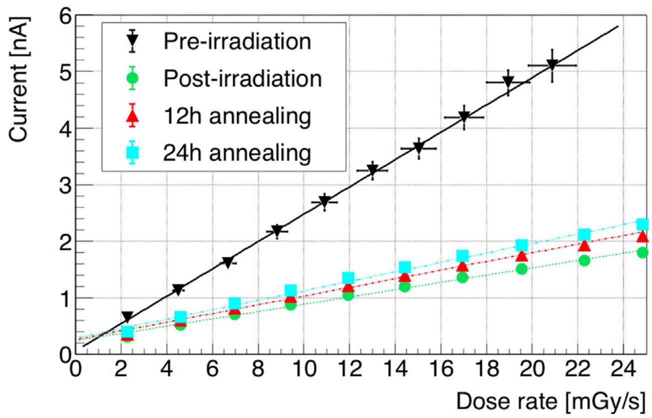

Fig. 13. Configuration (a) device response to x-ray irradiation versus dose rate. The measurement where taken before and after neutron irradiation and after 12 and 24 h of annealing at 100 °C.

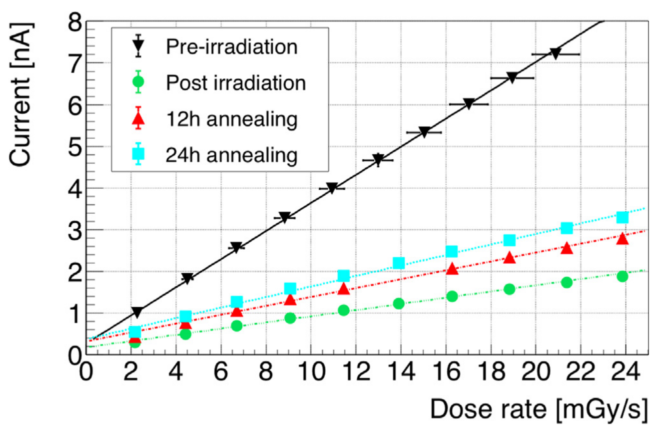

Fig. 14. Configuration (b) device response to x-ray irradiation versus dose rate. The measurement where taken before and after neutron irradiation and after 12 and 24 h of annealing at 100 °C.

Table 2
Sensitivity under various conditions for configuration a and b devices after 5×10^{16} neq/cm^2 neutron irradiation.

Detector type and bias	Pre-rad Sensitivity (nC/cGy)	Sensitivity after irradiation (nC/cGy)	Sensitivity after 12h annealing (nC/cGy)	Sensitivity after 24h annealing (nC/cGy)
Configuration a device at 60V bias	1.94 ± 0.07	0.568 ± 0.005	0.769 ± 0.006	0.837 ± 0.006
Configuration b device at 60V bias	2.55 ± 0.08	0.737 ± 0.006	1.07 ± 0.01	1.27 ± 0.01

4. Conclusions

A total of four a-Si:H detector devices have been irradiated with neutron at the Jozef Stefan Institute reactor facility in Liubljana (SLO). These detectors were designed in three different configurations:

- **Configuration a:** Vertical p-i-n diode devices in square pads (0.5 mm × 0.5 mm).
- **Configuration b:** Vertical p-i-n diode devices in strips (5 mm × 0.2 mm)
- **Configuration c:** Vertical diodes with charge selective contacts in square pads (4 mm × 4 mm)

One device of configuration (b) and one configuration (c) were irradiated up to the total fluence of 1×10^{16} $n_{eq(1MeV)}/cm^2$ and then annealed for 12 h (device type (b) and (c)) and 24 h (device (c) only) at the temperature of 100 °C. After the irradiation, we observe an increment in leakage current, more homogeneous at all bias voltages for configuration (c) device and more evident at low bias voltages for configuration (b) device. After 12 h of annealing, the leakage current returned to the original value for the configuration (b) component and was reduced to about 50% for the configuration (c) device. The radiation sensitivity under non-zero bias was reduced by more than a factor of 2 after irradiation and partially recovered (up to 65%) for the charge selective contact device and had a 25% increment compared to the original value for the configuration (b) device. From these results, we can infer that irradiation generates relevant damage in the two devices. After annealing, we observe a full recovery of leakage current and a partial (on CSC devices) or total (on p-i-n devices) recovery of radiation sensitivity. Concerning the irradiation of one configuration (a) and one configuration (b) device up to fluences 5×10^{16} n_{eq}/cm^2 it is important to consider that due to activation the two devices were measured only after 146 days from the end of neutron irradiation and these may have induced some self-annealing making the successive 100 °C annealing less efficient in the recovery of the performances. Nevertheless, the two devices, after 24 h of annealing, recovered partially their performances. The radiation sensitivity, after the complete annealing process was 43% of the pre-rad value for configuration (a) and 50% for configuration (b). In the near future we plan to repeat the irradiation with protons in the few MeV energy range, combining the effect of displacement with the effect of the total ionizing dose. An investigation of the damage mechanism caused by neutron irradiation is beyond the scope of the present paper which is focused to functional measurements in beam monitoring applications. A dedicated paper on this topic has been published and it reports structural analysis based on soft X-rays high resolution photoemission spectroscopy and atomic force microscopy [14]. The main results of this work are that neutron irradiation causes the decrease of Si-H bonds and an increase of dangling bonds in the active material. This causes an increase defects in the bandgap increasing the leakage current and decreasing charge collection efficiency (even in the long term) leading to the observed reduction in dosimetric sensitivity. It was also observed that the number of Si-H bonds tend to increase after annealing generating a partial recovery in terms of reduction of leakage current and increase of dosimetric sensitivity.

Declaration of competing interest

The authors declare that they have no known competing financial interests or personal relationships that could have appeared to influence the work reported in this paper.

Data availability

Data will be made available on request.

Acknowledgments

The authors wish to acknowledge the JSI personnel in particular Dr. Anze Jazbec and Dr. Matjaz Mihelic for their fundamental contribution during activation monitoring and X-ray tests. The p-i-n devices were developed by Fondazione Bruno Kessler (FBK) in the framework of FBK and INFN MiNaTAP agreement on an a-Si:H layer deposited by EPFL. Charge selective contacts devices were fully developed by EPFL. For this project, Matthew Large is sponsored by the AINSE Post Graduate Research Award (PGRA) – Australia, and is supported by the Australian Government Research and Training Program (RTP) scholarship. The project was Funded by the CSN5 of INFN under the grants: 3D-SiAm and HASPIDE. Additional funds came from the "Fondazione Cassa di Risparmio di Perugia" RISAI project n. 2019.0245.

References

[1] J.R. Srour, et al., Damage mechanism in radiation-tolerant amorphous silicon solar cells, IEEE Trans. Nucl. Sci. 45 (1998) 2624–2631.
[2] J. Kuendig, et al., Thin film silicon solar cells for space applications: Study of proton irradiation and thermal annealing effects on the characteristics of solar cells and individual layers, Sol. Energy Mater. Sol. Cells 79 (2003) 425–438.
[3] H.C. Neitzert, et al., Investigation of the damage as induced by 1.7 MeV protons in an amorphous/crystalline silicon heterojunction solar cell, Sol. Energy Mater. Sol. Cells 83 (2004) 435–446.
[4] N. Wyrsch, et al., Radiation hardness of amorphous silicon particle sensors, J. Non-Cryst. Solids 352 (2006) 1797–1800.
[5] M. Menichelli, et al., Hydrogenated amorphous silicon detectors for particle detection, beam flux monitoring and dosimetry in high-dose radiation environment, JINST 15 (2020) C04005.
[6] M. Menichelli, et al., 3D detectors on hydrogenated amorphous silicon for particle tracking in high radiation environment, J. Phys.: Conf. Ser. 1561 (2020) N.012016.
[7] M. Menichelli, et al., Fabrication of a hydrogenated amorphous silicon detector in 3-D geometry and preliminary test on planar prototypes, Instruments 5 (2021) N. 32.
[8] M. Menichelli, et al., Testing of planar hydrogenated amorphous silicon sensors with charge selective contacts for the construction of 3D detectors, JINST 17 (2022) C03033.
[9] N. Wyrsch, C. Ballif, Review of amorphous silicon based particle detectors: The quest for single particle detection, Semicond. Sci. Technol. 31 (2016) 103005.
[10] G. Lindstom, Radiation damage in silicon detectors, Nucl. Instrum. Methods Phys. Res. A 512 (2003) 30–43.
[11] A. Jazbeck, Private communication, 2021.
[12] 2022. Datasheet available at http://www.newtonscientificinc.com/50kv-10w-monoblock/. (Last Accessed 23 June 2022).
[13] 2022. Specifications available at https://rtigroup.com/products/cobia/rti-cobia-flex-r-f/#specification. (Last Accessed 23 June 2022).
[14] F. Peverini, et al., High resolution photoemission study of neutron induced defects on hydrogenated amorphous silicon devices, Nanomaterials 12 (2022) 3466.